Image Analysis by Granulometry Morphological Opening on Rat liver Vessel's During Bile Duct Ligation

Isamaldin H.S.Badawi1A. G. Afadil 2, and Alfredo Colosimo3
Department of Biomedical Physics, Faculty of Science and Technology, Al-Neelain University, Khartoum, Sudan.
Department of Environmental Science, Faculty of Science and Technology, Al-Neelain University, Khartoum, Sudan.
Department of Biomedical Physics, Faculty of Science and Technology, Al-Neelain University, Khartoum, Sudan.
alfabme@gmail.com

Abstract

A logarithmic granulometry image analysis was developed by morphological opening on (SEM) images of rat liver; we applied the granulometry analysis on different images of micro-vessel's corrosion cast to determine the surface area (SA), first derivative surface area (FDSA). The results tested by probability density function (PDF) theory, kernel smoothing density estimate (KSD), using analysis of multi-variance (ANOVA-two ways) to determine alteration changes on the micro-vessels during experimental induced cirrhosis by Bile Duct Ligation (BDL) in liver, the investigation improve better understanding vessels morphology from vascular corrosion cast and morphogenesis during cirrhosis by (BDL). The investigation prove and measure the alterations of the ratio Surface Area of vessel's to Surface Area space between vessel's, therefore ratio (SA/FDSA) of the surface area over first derivative surface area prove the alteration during cirrhosis by (BDL).

Keywords: Granulometry, Mathematical Morphology, Image Opening, Probability Density Function, Kernel Smoothing Estimation, Surface Area, First Derivative Surface Area, Bile Duct Ligation (BDL), Cirrhosis

Introduction

This paper mathematical and computational considerations concerning to size distributions by granulometry. Applying granulometry morphological opening and statistical theory to gain meaningful and measurable parameters for size distributions of micro structures of the rat liver during induced cirrhotic by bile duct ligation.

This paper clear proof that image analysis and processing by morphological functions granulometry increase, quantitatively and qualitatively information's about micro-vessels in cirrhosis by bile duct ligation, the data are SEM images of vessels corrosion cast. As background basis, the liver as an organ has major importance in a human body as one of the parts of digestive systems with supply of blood vessels organization to do more than 500 physiological functions in cyclic daily duty [Asrani et al, 2013]. In many researches about the liver cirrhosis have proven that common pathological pathway causes the liver damage comes from variety factors of the chronic liver diseases [Melato and Mucli, 1989],[Qua and Goh, 2018]and [Zhou et. Al, 2019]. Chronic hepatic failure is the more common and progressive form of the disease. The definition of Cirrhosis is a degenerative process in the liver marked by excess formation of connective tissue destruction of functional cells and often contraction of the organ [Galletti and Jauregui, 2013]. On the definition, nomenclature, and classification of cirrhosis, chronic hepatitis, and hepatic fibrosis, considered according to morphological characteristics and aetiology to provide guidelines for the pathologist on the definition [Anthony et al ,1978].

The mechanisms of hepatic micro-circulation regulation depend on the hepatic microvasculature input blood from two types of afferent vessels. The terminal portal venule directly connected with the capillary bed in the liver parenchyma, which is referred to as sinusoid. Hepatic arterial blood pours into the hepatic sinusoid not only indirectly via the anastomosis between the terminal hepatic arteriole and the portal venule [Oda et. al., 2003]. The study of the morphology of the hepatic circulation has given evidence that the liver consists of a large vascular delta formed by the confluence of the portal and arterial streams. Their arms, which subdivide the delta into lobar areas, start to run parallel and close to each other when they are still visible to the naked eye. Dwindled down to microscopic size, they become the scaffold of the parenchymal cell masses nestling between the microvessels, it is evident that vascular morphology is the visual aspect of the dynamic blood flow, thus permitting us to perceive its functional orderliness, and to study the circulatory physiology in the hepatic delta. The main measurement of hepatic blood flow methodological problems discussed [Rappaport, 1980].

About hepatic micro-circulation as a morpho-functional basis, is well known as a fundamental component the liver structure, deeply involved in the zonal organization of the acinar structure. In cirrhosis, the microvascular tree shows dramatic changes that would heavily influence the development of the disease. When the cirrhosis becomes evident the result is a progressive organ failure, this in presence of only moderately decreased hepatocytes volume [Gaudio et al, 1995]. Laparoscopic totally extraperitoneal (TEP) inguinal hernia repair in patients with liver cirrhosis accompanied by ascites, to investigate the feasibility efficacy and safety of laparoscopic [Wang et al 2019].

The empirical data from images to study induce cirrhosis in rat model support, increases scientific information's, functional change in the liver vascular during the morphological, physiological and pathological stages of the cirrhosis with the morphological measurable quantities [Gaudio et al, 1993]. The experiments to induce the cirrhosis in laboratory empirically, study progress of pathological alteration in the vessels or liver tissues using bile duct ligation (BDL) [Gaudio et al, 2005].

The method of corrosion casting has been known since the 16th century when Leonardo da Vinci made the first casts by injecting dissolved wax into bovine cerebral ventricles and heart chambers [Giuvarasteanu, 2007]. Anatomists improve the casting media, the method of injection, and the method of removing the surrounding tissues in order to produce more accurate replicate of the biological structures. The modern corrosion casting methods are based upon the idea of Jan Schwammerdam who in the late 17th century dissolved the surrounding tissues after wax injection into the arteries, veins and ducts [Giuvarasteanu, 2007].

The microvasculature technique of tissues and organs vascular corrosion casts (VCCs) enables to study and characterize by visual inspection in the scanning electron microscopy (SEM) during both normal and pathological conditions for animals and humans [Minnich and Lametschwandtner, 2010]. The vascular corrosion casts of the micro-vascular arrangement of the extra hepatic biliary tree of the rat was studied by light microscopy (L.M.) and scanning electron microscopy (S.E.M.) to observe plexus encircles in lumen of The common bile duct by LM and showed a network of vessels of different diameters with under the epithelium of the lamina propria [Gaudio et al, 2005]. In general to evaluate the performance of Collagen Proportionate Area (CPA) and ELF using Ishak's score in patients [Stasi et al, 2019].

Image analysis and image processing tool box within Matlab recently develop large amount of mathematical morphological functions to empower image analysis supported with standard algorithms, to perform features measurement and morphological structures in images, with less progress in calibration standardization, Therefore we carried this research with following objectives satisfy image analysis goal, which effect image processing and analysis on group of images perform statistical analysis, improve confidence we create algorithm of granulometry enclosed by morphological functions, the statistical functions for every single image on one execution, the result data stored as matrix spread sheet file.

Materials and Methods

We presents the methods have been used in paper, mathematical morphology fundamentals function that enters in the granulometry. The statistically test performed on the data of the image. The algorithm has been used to compile the granulometry. They are two types of functions have been used, a computer functions one as routine solutions of the mathematical functions itself and mathematical morphology are enclosed in Matlab library.

Morphological functions:

The background about mathematical functions, the mathematical morphology is a tool for extracting geometric information from binary and gray scale images, a shape probe is structuring element, references [Soille P., 2013; Castleman,1990; Doigherty and Lotufo, 2003].

The statistical analysis, fundamental functions are probability density function, kernel smoothing density estimate (ks-density) and Anova two ways.

Structuring elements (SE):

Structuring element essential part for morphological operations, the structuring element used to probe input image. The shape created by matrices with two values consisting of only zeros and ones. The ones is white pixel, and zeros is the black pixel, a structuring element is a matrix arbitrary shape and size. Two types are flat structuring element and non flat. The center pixel of the structuring element is origin identifies the pixel of interest processing; the pixels in the structuring element containing ones define the neighborhood for structuring element. The structuring elements is disk shape, see figure (1), with radius R where R is the non negative integer, and size N is values must be [0,4,6,8], in granulometry operation the N must not zero.

Dilation and Erosion:

Dilation and erosion are fundamental operations in morphological transformations, and many of the morphological algorithms based on these two operations. Dilation added pixels to the boundaries of objects in an image with complete values of image pixels tend to one bright image, while erosion removes pixels on object boundaries with full values of image tend to be zero dark images. The number of pixels added or removed from the objects in an image depends on the size and shape of the structuring element used to process the image [Jain A. K., 2015]

Opening and Closing:

Opening generally smooth the contour of an object, breaks narrow items, and eliminates thin protrusions. Closing tends to smooth sections of contours but, as opposed to opening, it is generally fuses narrow breaks and long thin gulfs, eliminates small holes, and fills gaps in the contour, the morphological close operation is a dilation followed by an erosion, fill the gaps of objects smaller than structuring element (SE) in the binary image it removes the dark and black objects smaller than structuring element (SE) in gray level image, image end to one pixel's white image.

Opening (γ) is defined as:

The opening of set A by structuring elements B, denoted $A \square B$ and $\gamma(A)_B$ is defined as

$$A \square B = (A \Theta B) \square B \qquad (1)$$

$$\gamma_B(A) = \delta_B(\varepsilon_B(A)) \qquad (2)$$

Closing (ϕ) is defined as:

The closing of set A by structuring element B, denoted A•B and $\phi(A)_B$ is defined as:

$A \square B = (A \square B) \Theta B$ (3)

$\phi(A)_B = \varepsilon_B(\delta_B(A))$ (4)

The most basic morphological operations are dilation and erosion, closing and opening. With symmetrical structuring element the particularities opening and closing have duality operations opening and closing are dual operations. Increasing the opening and closing are compositions of increasing operations of erosion and dilation, the opening and closing are also increasing; the opening is anti-extensive covering and affecting small area while the closing is extensive covering and affecting a large area. With the factor elements of set which not changed in values when multiplied or operated by itself. The opening and closing are idempotent operations applying them to an image twice give the same result as applying them only once.

Granulometry:

The granulometry mathematically with algebra formula defined as operation comes from the lattice space in physics and group theory, the granulometry based on sieving function $\boldsymbol{\psi_\lambda}$ with increasing the grid size of lattice is **λ>0,** by applying sieving λ on any set. The concept of granulometry was introduced by G. Matheron at 1967 [Matheron, 1967], the family set $\{\gamma_\lambda\}$ of opening operation depends on positive parametric factor grid size or structuring element size λ when increases proportionally to each others with considered condition $(\lambda \geq \mu > 0) \rightarrow \gamma\lambda \leq \boldsymbol{\gamma_\mu}$ the computed values element λ summation when plotted composed curve is the distributional function of the total granulometry.

$F_\lambda = (1 - M_\lambda / M_\lambda)$ (5)

Granulometry with mathematical morphology is define in steps and generated by a structuring element B in Euclidean space E, the set of all size of B is $\{B_k\}$where k =0,1,2,3,...., arranged in the equation: $B_k = B_1 \square B_2 \square .... \square B_{k+1}$, k is the repeating of the $\square$morphological dilation, if the binary image is set of $\{X\}$, the series of sets is $\{\gamma_\mu (X)\}$,k=0,1,....operation given by equation (6):

$\gamma_k (X) = (X) \square B_k$ (6)

The granulometry in equation (7) is the function $G_k(X)$ is the set of all measurable in the image set $\{\gamma_k (X)\}$ and numbers of element in the grid,

$G_k(X) = |\gamma_k (X)|$ (7)

The size distribution and pattern spectrum of granulometry is:

$PS_K (X) = G_k(X) - G_{k+1}(X)$ (8)

Where k =0,1,2,…,is size of element in the components of $PS_K(X)$ make rough estimate object size [Matheron, 1975; Serra J., 1982].

Surface area, first derivatives in granulometry:

Theoretical comparison of the surface area in granulometry geometry with classical geometry, the summation of the granulometry operation with structuring element disk or circle is surface area then with differentiation function the relationship between the area A of a circle with radius r and its circumference P can be expressed as:

$A'(r) = (\pi r^2)' = 2\pi r = P(r).$ (9)

The a relationship of this a derivative between the area and the circumference or perimeter of a circle, the derivative relationship is best seen geometrically Fig.(1). When the radius of the circle is extended from (r) to (r + h), the area of the circle changes by ($\Delta A = 2\pi rh + \pi h^2$), which is the area of the ring of width h around the circle of radius (r) when (h) approaches zero, the ring approaches the inner circle.

In Matlab the differences and approximate derivatives gives by solving in equation (11) for every single granulometry components, if Y = diff (X), calculates differences between adjacent elements of X.

The differences between adjacent elements give as:

Diff (X)=[X(2) - X(1)X(3) -X(2)...X(n) - X(n -1)] (10)

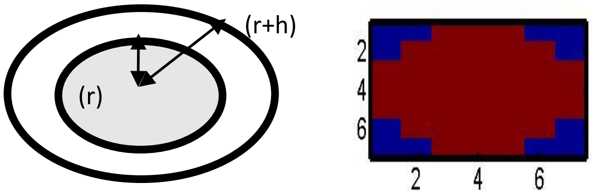

Fig(1) the circumference perimeter and area relationship with structuring elements circles and disk changes in their diameters during the operations of granulometry, where r is radius, h is increasing in the radius.

Statistical distribution functions:

To perform statistical distribution with statistical toolbox in Matlab and analyze large amount of data supporting by granulometry algorithm from the images to determine with accurate measurable particular differences in the stages cirrhotic images of scanning electron microscope, the function is kernel smoothing density estimate (ksdensity) as statistical analysis. The data saved in file to more invstigate by advance nonparametric statistical analysis with probability density function, and Anova two way functions as second analysis of variance.

Kernel smoothing density estimate (ksdensity):

In statistics, kernel density estimation (KDE) is a non-parametric way to estimate the probability density function of a random variable, ksdensity

$$\hat{f}_h(x) = \frac{1}{n}\sum_{i=1}^{n} K_h(x - x_i) \quad = \frac{1}{nh}\sum_{i=1}^{n} K\Big(\frac{x - x_i}{h}\Big), \quad (11)$$

as function computes a probability density of the samples x. [Bowman and Azzalini,1997].

Where is x data of granulometry surface area and first derivative surface area (x) where (f_h) is vector of density values evaluated at the points (x_i). K_h is the kernel a symmetric but not necessarily positive function that integrates to one, and h>0 is a smoothing parameter called the bandwidth. A kernel with subscript h is called the scaled kernel and defined as $K_h(x) = 1/hK(x/h)$. Where K is kernel smoothing function [Baumann and Tinembart, 2005].

Probability density normal distribution function (pdf):

With Matlab Statistics Toolbox provide functions with distributions, the most useful one is the probability density function (pdf), cumulative distribution function (cdf) and mean and variance as a parameters [Bowman and Azzalini,1997]. In equation (12) y-axis is the probability density of the function f of the data x, σ is the standers deviation, σ^2 is variance, μ is the mean, median and mode, e is natural algorithm e =2.0149 [Baumann and Tinembart, 2005].

$$y = f(x|\mu,\sigma) = \frac{1}{\sigma\sqrt{2\pi}} e^{\frac{-(x-\mu)^2}{2\sigma^2}} \quad (12)$$

Anova two way and multi compare analysis:

The analysis of variance (ANOVA) refers to a collection of experimental situations and statistical procedures for the analysis of quantitative responses from experimental units. ANOVA used for comparing means of Data sampled from more than two populations. Also Data from experiments in which more than two treatments have been used [Polikar R.,2016]. Anova (two-way) is a procedure for assigning sample variance to different sources and deciding whether the variation arises within or among different population groups. Samples are described in terms of variation around group means and variation of group means around an overall mean. If variations within groups are small relative to variations between groups, a difference in group means may be inferred. Hypothesis tests are used to quantify decisions. Anova two-way analysis of variance for data don by Matlab. The variability due to the differences among the column means of data. The variability due to the differences among the row means data. Variability due to interaction between rows and columns, The remaining variability not explained by any systematic source [Hogg and Ledolter, 1987].

Granulometry algorithm:

This article the main methodology is granulometry algorithm by Matlab, Image processing toolbox, and statistical tool box function probability density function and kernel smoothing functions as part of the statistical test in Matlab. The mathematical morphology functions in Matlab rise wide broad new classes open up applications in image analysis, segmentation and enhancement. The basic main functions existing are dilation and erosion with structuring elements operators that extend with binary and gray scale images. The functions range from morphological opening and closing useful for segmentation, distance transforms, reconstruction-based operators, and the watershed transform. The functions use advance techniques for high performance, including granulometry with mathematical morphology functions based algorithms. The Matlab image processing tool functions reading image different type of image from different medical modalities the major one electron microscopy images. The Algorithm granulometry is described [Ronald and Soille, 2018], the Algorithms as in blocks of Fig (2)

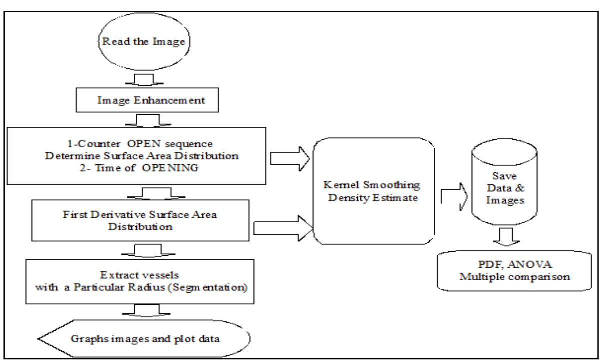

Fig. (2) The flow chart of the granulometry.

Result and Discussion

The results obtained from the granulometry algorithm from rat liver vessels during stages of cirrhosis by bile duct ligation. The discussion in two parts one on the results perform on the images and their complements, the second part about the comparison with other results obtained.

Liver bile duct ligation cirrhosis images:

Basic liver architecture unit is hexagonal lobule, composed of blood vessels, portal vein and hepatic artery and hepatic bile duct, they communicate with the liver at the hilus, then branch within the liver to form a system that travels together in a conduit structure, the portal canal then branching, the portal vein drains into the sinusoid, which is the capillary system of the liver with (8-10) µm diameter. The liver cirrhosis images to obtain quantitative and qualitative results of scanning electron microscope (SEM) corrosion cast VCCs of cirrhotic and control rat livers of Male Wistar rats. The images of BDL-inducing cirrhosis, the bile duct was double ligated and then sliced animals were killed 2 and 4 weeks after BDL, standard magnification of x 80, the image (A-ctrl) is the control near and far from the hilus, the image (B-BDL 2 W) is taken 2 weeks after bile duct ligation, the image (C-BDL 4 W) taken 4 weeks after bile duct ligation results obtained in [Gaudio et al, 2005].

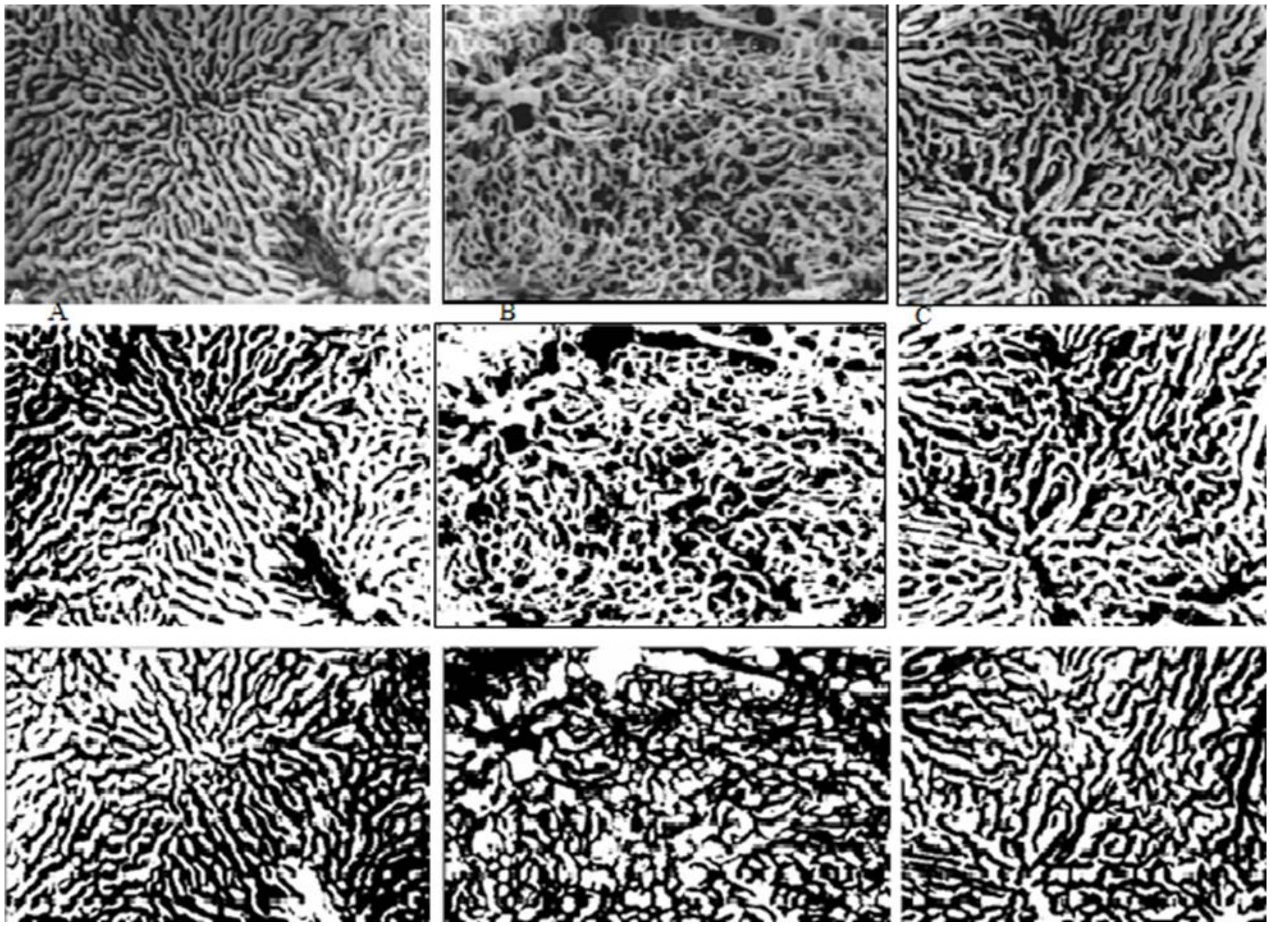

Fig.(3) From upper left images (VCC), A control healthy vessels, B-BDL after 2 weeks, C-BDL after 4 weeks. A second row are binary image of first row, the third row is complement (negative) images of second row

The granulometry morphological opening

To create very high accuracy and error-less on the granulometry algorithm, we have been justify, correct, calibrate images by the main factors that effects on the images processing, the images size have been equalized, the image type unified as binary, the images restored by histogram equalizer, the intensity of light pixel's justified. The structuring element is disk geometrical shape used in all images. In is this part, the results presents in two groups of images, one is the surface area and first derivative surface area of the vessels, the second group is complement images to determined the surface area and first derivative surface area for the space between vessels and the hepatic sinusoidal. The main results divided in two categories Group (1) for vessels: Surface area (SA), and first derivative surface area (FDSA), kernel smoothing estimation of (SA) and (FDSA). The second is Group (2) for space between vessels and hepatic sinusoidal: Surface area (SA) and First derivative surface area (FDSA). Kernel smoothing estimation of surface area (SA) and first derivative surface area (FDSA). Anova two way statistically comparisons test on both two groups

The surface area and First derivative surface area of the vessels Group (1):

From the images of binary in figure (3) obtained the results, we presents in illustration. In Fig.(4) presents different curves of granulometry of the surface area (SA) of the vessels by function open, the y-axis is the process of the summing pixels generated from opened vessels, the control of the steps is structuring element (SE) with disk shape, the y-axis range from(8) -(12)□10^5μm^2. The x-axis is the radius of opening same time is the structuring element size, the size begins from zero to 35, with units of pixel per micro meter. The total operation of granulometry by opening ends to zero pixel values, descending from maxim to minim. At the levels of small size of structuring elements the curves are presents likelihood, with moderate variation after middle size. The Radius of opening is accuracy identical size of the diameters of the vessels from size zero to size 5, this phenomenon can determine the vessels diameters in the beginning of granulometry.

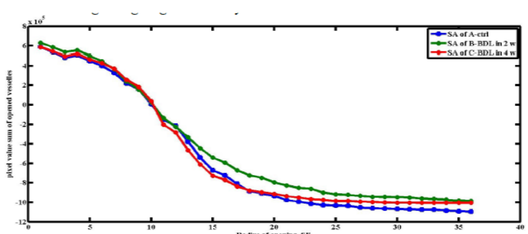

Fig.(4) Surface area (SA) granulometry opening vessels group(1), y-axis the summations opened vessels steps depend on structuring element(SE) disk shape, x-axis is the radius of opening, healthy vessels blue, bile duct in two weeks in green, bile duct in four weeks in red.

In figure (5) the first derivative of the surface area group (1) by differences and approximate derivatives of the surface area data during granulometry opening, y-axis is the FDSA by sum of pixel in vessels as function of radius and diameter of the vessels the range is from (0.5) to (-.25)□10^5 μm, x-axis the vessels radius and structuring element size range from zero to 35 SE. The curves of granulometry FDSA is type of spectrum curves distribution, show the variation during operation of opening. The FDSA is very small size than SA. A significant variation in FDSA between two consecutive openings is indicates that image contains objects of comparable size to the smaller opening. The above variation is useful to segmentation and separation of the large vessels from small vessel in demands of vessels diameters.

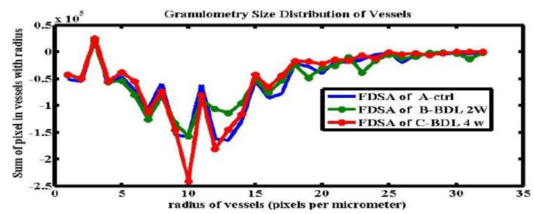

Fig.(5) First derivative surface area group (1), y-axis FDSA sum of pixel's in vessels as function of radius, x-axis radius of the vessels.

After the SA and FDSA processed we have perform mathematical analogue due to surface area over derivative surface area relation, divided the SA over FDSA as matrix operation in Matlab, the result presents in figure (6). In figure (6) shown the ratio of surface area over first derivative surface area of the group (1), y-axis is the SA/FDSA vessels as function of radius, x-axis is the radius of the vessels. The result of comparison of (SA / FDSA) with clear variability in two points in x-axis, radius size from zero to 10 SE micrometers, C-BDL4W is large size then A-ctrl, B-BDL 2 W. The second point from 10 to 35 SE micrometer shows that the A-ctrl is greatest size then B-BDL 2 W, and C-BDL 4 W. The interpenetration that granulometry in small size of SE comparing small objects (vessel's) in the images, and large objects (vessel's) comparable in large size of SE.

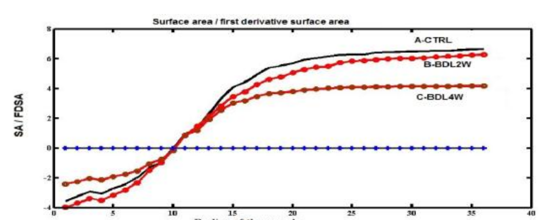

Fig.(6) Ratio of surface area over first derivative group (1), y-axis is the SA/FDSA vessels as function of radius, x-axis is the radius of the vessels.

Comparing SA Vs FDSA for the vessels:

In Figure (7) shown as box-plots the surface area verses the first derivative surface area, the comparable between the both SA and FDSA gives accuracy of the granulometry, the surface area is comparatively larger than first derivative surface area, y-axis range from (6) to (-12)□10^5µm, the ratio SA:FDSA is about (2:8)□10^5 µm. The Boxes plots central mark is the median by red colors, the edge is the stander deviation by T-shape dots represents the tail of data, the red dots out of the boxes is data out of the range statistically. The boxes show the data of granulometry is statistically accepted values. Variation between SA versus FDSA, surface area is greater than first derivative by ratio of (2:8), is significant and strong proof of granulometry characteristics as morphology tool, applied directly in different images type in clinical and researches [Velleman,Hoaglin,1981], Nelson,1989,]and [McGill et al,1978].

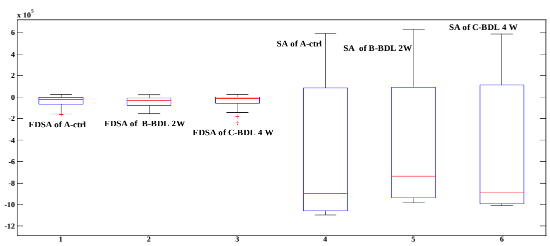

Fig.(7) comparison vessel's surface area against first derivative surface area by box-plots, the small boxes group FDSA while grand boxes represents SA.

Kernel smoothing estimation the SA and FDSA of the vessels:

In figure (8) Kernel smoothing estimation by (Ksdensity) in Matlab statistical tool box function, The y-axis is Probability density verses data of surface area distribute in x-axis the granulometry surface area depends of radius size. The curves are Bi-modality type for SA probability density, SA with large size of diameters and structuring elements on x-axis in range between (1 to -0.5), the small size of diameter in range between(-0.5 to -1.5) largest peak, small size surface area vessels in identical to the diameters of structuring element. The maximum largest size is SA B-BDL2w of bile duct in two weeks red color, A-healthy control in blue color and C-bile duct ligation in four weeks in brown color. In C-BDL 4 w in x-axis from 0.5 to -1.5, peak have smallest full width at half maxim, means the vessel's start to reshape compacted longitudinal organization.

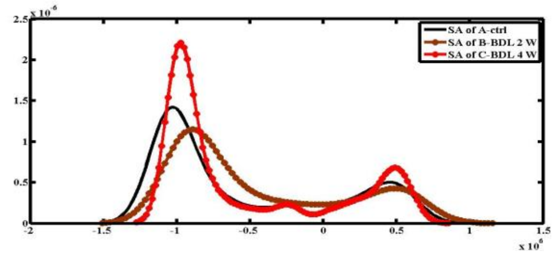

Fig.(8) Probability density surface area, healthy control in black color, bile duct ligation after 2 weeks in brown and the red is bile duct ligation in 4 weeks, curves are bi-modality type, from 0.5 to -1.5 represents small SA and SE, and from 1 to -0.5 on right represents large size of SA and SE. The FDSA of the bile ducts ligation in two weeks (B-BDL 2 w) is comparable with other two curves is undifferentiated diameters of vessel's. The maximum largest size is FDSA of bile duct in two weeks curve with red color, the A-healthy control in blue color and C-bile duct ligation in four weeks in brown color.

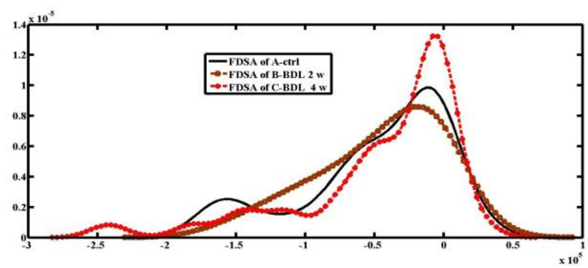

Fig.(9)Probability density first derivative surface area A-healthy control black color, B-bile duct ligation after 2 weeks brown and red C-bile duct ligation in 4 weeks.

The SA and FDSA space between vessels:

In this group (2), granulometry analysis performed on the complemented negative images of the vessels corrosion cast to determine morphological parameter of the surface area and first derivative surface area. The main target is to determine the SA and FDSA for the hepatic cells and hepatic sinusoidal space, that have been filling the same space between vessel's, the cells have been removed during corrosion cast process and washed out. The curves on figure (10) illustrate both surface area and first derivative surface area, figure (10.A) presents the SA for the space between vessel's and hepatic sinusoidal space, the y-axis range from zero to (14)□10^7μm.^2, the x-axis represents the structuring element and diameters of the space between vessel's.

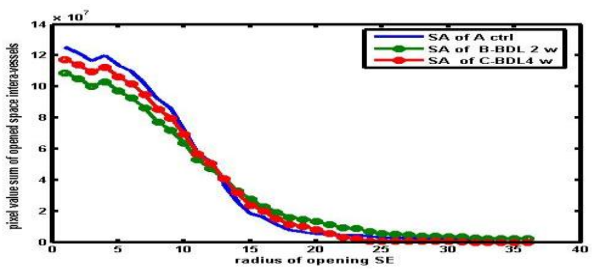

Fig.(10.A) Plot surface area, healthy control in blue color, bile duct ligation after 2 weeks in green and the red is bile duct ligation in 4 weeks.

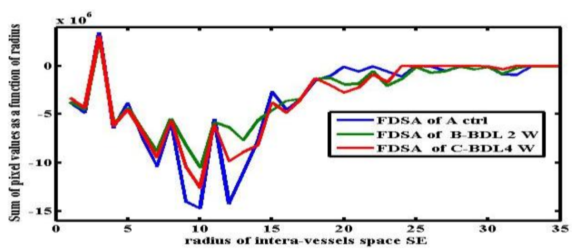

Fig (10.B) FDSA space between vessel's, y-axis range from zero to (14)□10^7μm.^2, x-axis represents the structuring element diameters of space between vessel's.

The comparing of ratio of surface area against first derivative surfaces area space between vessel (hepatic sinusoidal space) of bile duct ligation have been performed, by dividing SA over FDSA as matrix operation in Matlab, the illustrate in figure (11) present the results, the result shown the variation of the SA/ FDSA decreasing from A-ctrl of normal healthy, C-BDL in 4 weeks and B- in 2 weeks respectively in all size of radius during all stages of granulometry, in clear as crystal to proof the power full of granulometry, and hepatic sinusoidal space variability in radius size and (surface area : surface area derivative area) during stages of bile duct ligation's.

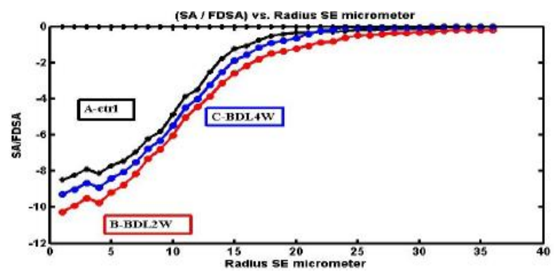

Fig.(11) Ratio of surface area over first derivative surface area of group (2) space between vessel's, y-axis SA / FDSA vessels as function of radius, x-axis is the radius of the vessels.

Comparing SA Vs FDSA space between vessels:

The comparative investigation performed to the data of SA verse FDSA as two group the group of vessel's and group of space between vessel's, which have been removed during space corrosion cast process for the hepatic sinusoidal, the comparison output with unique variations values between surface area verse first derivative, the variably differences shown as box-plots in figure(12), the range of vertical axis from zero to 12□10^7, the horizontal axis is the two types of data.

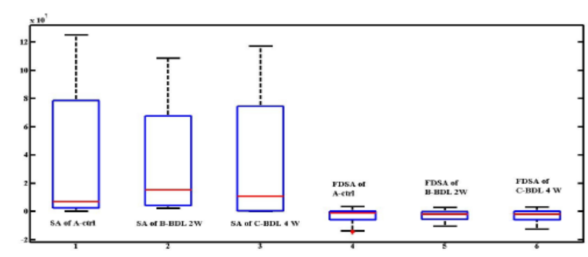

Fig.(12) The comparison of data, on left SA while the boxes on right represents FDSA space between vessel's.

Kernel smoothing estimation for SA and FDSA the space between vessels:

In this part presents the output performance of probability density by kernel smoothing estimation method for the data of the both SA and FDSA. In figure (13) the y-axis is the probability density in range from zero to 4×10^{-8}, while the x-axis is the SA data, the curves are bimodal type with two groups of maximum peaks, the great peak representative for the small size of structuring element diameters directly, in same time indirectly is the diameters of the space between vessel's (hepatic sinusoidal space). From central maximum peak point between 2 to -2 in x-axis, the curve of healthy control in dark black color is greatest and largest size of surface area, the C-BDL after four weeks in second order and B-BDL 2W surface area of bile duct litigation in two weeks in the middle. With shift towards right in interval range between -2 to 2 the B-BDL 2 W means that the surface area is smallest size

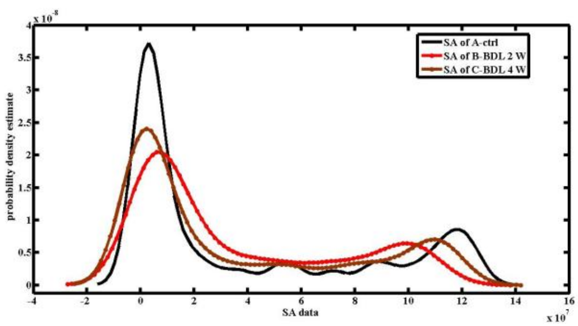

Fig.(13) SA space between vessel's depends on radius decrease from A-ctrl, B-BDL 2 W and C-BDL 4 W respectively, x-axis max peak represent small structuring elements SE.

In figure (14) the y-axis is the probability density in range from zero to 2.5×10^{-7}, while the x-axis is the FDSA data, the curves are bimodal type with two groups of maximum peaks, the great peak representative for the small size of structuring element diameters directly, in same time indirectly is the diameters of the space between vessel's. From central peak between 0.5 to -0.5 in x-axis, the curve of healthy control in black color is greatest and largest size of FDSA, then B-BDL 2W in second order and FDSA of C-BDL 4 weeks. With shift to towards right in interval range between -0.5 to 1.2 the curve of C-BDL 4 weeks is the smallest size and the FDSA have no any differences between diameters as groups.

Anova two-way and multiple comparison test vessel's Vs Intra-vessel's

To investigate more morphological characteristics for the vessel's during bile duct ligation, we perform statistical analysis of variance by Anova two way method, between the group of vessel's and space between vessel's (hepatic sinusoidal space). Anova two-way performs a balanced comparing the means of surface area as columns and structuring element size of granulometry as rows of the total observations. Anova two-way analysis of variance for surface area vessel's against intra-vessel's data.

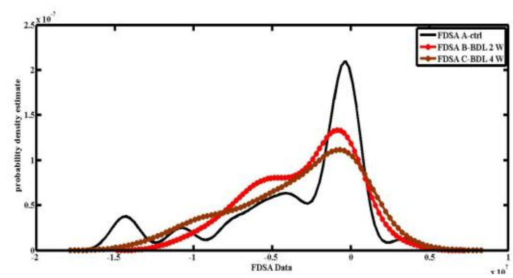

Fig.(14) FDSA space between vessel's, decreasing from A-ctrl, B-BDL 2 W and CBDL 4 W respectively the largest peak between 0.5 to -0.5.

The results in figure (15) shown significant variability among the two main groups surface area vessel's against surface area space between vessels. The surface area of the space between vessel's have largest size more than vessel's, means by cause and effect, causality the emptiness surface area of the space between vessel's is direct indication of the hepatic cells, this gap or free zone of the hepatic cells create the morphological changes on the vessel's. Table (1) presents the results of Anova two way, column 1 is source of the variability, 2 is sum of squares SS due to each source, 3 is degrees of freedom df associated with each source, 4 is mean squares (MS) which is the ratio SS/df, 5 is F statistics, which is the ratio of the mean squares and 6 is p-values

The Anova two-way analysis of variance for first derivative surface area vessel's against space between vessel's data. The Anova two way results in figure (16), the plots presents first derivative surface area in space between vessels is significant great than first derivative surface area of the vessels. The Anova two-way analysis of variance for first derivative surface area vessel's against space between vessel's data. The Anova two way results in figure (16), the figure plot presents first derivative surface area in space between vessels is significant greater than first derivative surface area of the vessels.

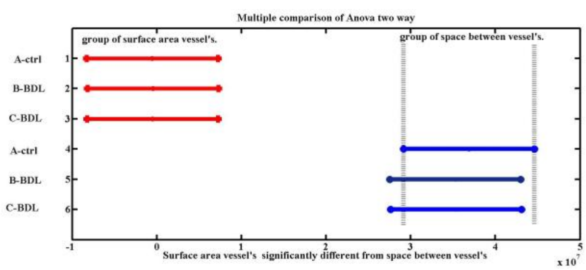

Fig.(15) Anova two way of surface area granulometry opening vessel's Vs space between vessel's.

Table (1) Anova two ways for surface area

Source	SS	df	MS	F	Prob>F
Columns	7.1e+16	5	1.4e+16	26.8	4.3e-20
Rows	9.6e+16	35	2.7e+15	5.2	8.6e-14
Error	9.2e+16	175	5.3e+14		
Total	2.6e+17	215			

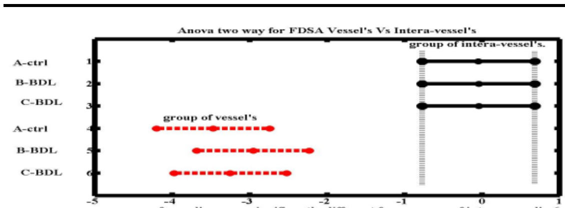

Fig.(16) Anova two way test for first derivative surface area granulometry vessel's against space between vessel's (hepatic sinusoidal space) y-axis data max is 4□10^6.

Table (2) Anova two-way for the granulometry first derivative surface area

Source	SS	df	MS	F	Prob>F
Columns	5.5e+14	5	1.1e+14	23.56	4.5e-18
Rows	7.8e+14	35	2.2e+13	4.77	1.8e-12
Error	8.2e+14	175	4.6e+12		
Total	2.1e+15	215			

Recommendations

We recommended the method of granulometry as morphological method permits accurate measurement to the vessels surface area, derivative surface area between vessels with excellent management of the images

We recommended the advantages to visualize output for morphological study, granulometry have accurate curves for images of different medical field consequently reliable can employed morphological and morphogenesis features changes.

We recommended the kernel density estimation and probability density to support granulometry investigate to gain more reliability, repeatability and accuracy.

Conclusion

In conclusion, granulometry analysis with morphological open to determine the morphological change during the bile duct ligation experiment induced cirrhosis has been significant resulted, statistically tested. The experiment of bile duct ligation effects initially on the surface area of the space between vessel's and space between vessel's, which have been removed during corrosion cast process, the effects start on hepatic sinusoidal and hepatic cells. Then succeeding affects the vessels.

The surface area of space between vessels is larger and greater than vessels during stages of bile duct ligation cirrhosis this fact support that cirrhosis by bile duct ligation begins to make effect firstly on the hepatic cells secondly affect the morphology on the surface area of the vessels.

The great significant variability among the two main group's surface area and first derivative surface area is indication for the morphological characteristics of granulometry analysis and the power full of the bile duct ligation to induce the cirrhosis stages.

REFERENCES:

[Anthony et al ,1978], P. P. Anthony, K. G. Ishak, N. C. Nayak, H. E. Poulsen, P. J. Schuer, And L. H. Sobin, (1978), The morphology of cirrhosis, Recommendations on definition, nomenclature, and classifcation. Journal of Clinical Pathology, 31, 395-414.

[Asrani et al, 2013], Asrani SK, Larson JJ, Yawn B, Therneau TM, Kim WR., (2013). Underestimation of liver-related mortality in the United States, Gastroenterology, 145(2):375-82.

[Baumann and Tinembart, 2005], Damien B. And Jacques T., (2005). Designing Mathematical Morphology Algorithms on FPGAs: An Application to Image Processing, Springer Berlin Heidelberg,Berlin, Heidelberg, isbn:978-3-540-32011-1.

[Bowman and Azzalini,1997], Bowman A. W. and A. Azzalini, (1997). Applied Smoothing Techniques for Data Analysis, the Kernel Approach with S-Plus Illustrations, Oxford University Press,17(10):1057- 1063.

[Castleman,1990], Castleman, K.R., (1990), Digital Image Processing, Prentice Hall.

[Doigherty and Lotufo, 2003], Doigherty E.R. and Lotufo,R.A, (2003), Hands On Morphological Image Processing, SPIE Press.

[Galletti and Jauregui, 2013], Galletti P. M., Jauregui, H.O., (2013). Liver Support Systems The Biomedical Engineering Handbook: Second Ed. Joseph D. Bronzino Boca Raton: CRC Press LLC.

[Gaudio et al,1993], Gaudio E, Onori P, Pannarale L, Marinozzi G., (1993). Natural Micro circulation of the extrahepatic biliary tree: A scanning electron microscopy study of corrosion cast, J. Anat.,182: 37–44.

[Gaudio et al, 1995], Gaudio E, Pannarale L, Franchitto A, Onori P, Marinozzi G., (1995). Hepatic microcirculation as a morpho-functional basis for the metabolic zonation in normal and pathological rat liver. Ital J Anat Embryol., 100 Suppl 1:419-28.

[Gaudio et al, 2005], Gaudio E., Chaberek S., Montella A., Pannarale L., Morini,S., Novelli G., Ostrowski K., (2005). Natural Fractal and Fourier analysis of the hepatic sinusoidal network in normal and cirrhotic rat liver, J. Anat.,207(2): 107–115.

[Giuvarasteanu I, 2007] Ileana Giuvarasteanu,(2007), Scanning electron microscopy of vascular corrosion casts standard method for studying microvessels, Romanian Journal of Morphology and Embryology, 48(3):257–261

[Hogg and Ledolter, 1987] Hogg R. V., and J. Ledolter. Engineering Statistics. New York: MacMillan, 1987.

[Jain A. K., 2015], Jain A. K., (2015). Natural Fundamentals of Digital Image Processing, Amazon, isbn 13: 978-0133361650.

[Serra J., 1982], Jean Serra, (1982). Image Analysis and Mathematical Morphology, Academic Press, London,UK, isbn:0-12-637240-3.

[Matheron, 1967] Matheron G., (1967), Eléments pour une théorie des milieux poreoux. Mason,Paris.

[Matheron, 1975], Kingman J. F. C., G. Matheron, (1975), Random Sets and Integral Geometry,Bull. Amer. Math. Soc., no. 5, 844-847

[McGill et al,1978], McGill, R., J. W. Tukey, and W. A. Larsen. "Variations of Boxplots." The American Statistician. Vol. 32, No. 1, 1978.

[Melato and Mucli, 1989], Melato M. and Mucli E., (1989). Something new in liver cirrhosis epidemiology, Lancet, 2(8659):395-6.

[Minnich and Lametschwandtner, 2010], B. Minnich and A. Lametschwandtner, (2010), Scanning electron microscopy and vascular corrosion casting for the characterization of micro vascular networks in human and animal tissues, Microscopy: Science, Technology, Applications and Education.

[Oda et.al., 2003], Oda M, Yokomori H, Han JY, (2003). Regulatory mechanisms of hepatic micro circulation, Clin Hemorheol Microcirc,29(3-4):167-82.

[Nelson, 1989,], Nelson, L.S., Evaluating Overlapping Confidence Intervals, (1989) Journal of Quality Technology. Vol. 21, pp. 140-141.

[Polikar R., 2016], Polikar, R.,(2016), The Analysis of Variance ANOVA, Rowan University, Dept. of Electrical and Computer Engineering. Lecture 11,

[Qua and Goh, 2018], Qua CS. and Goh KL, (2018). Liver cirrhosis in Malaysia: peculiar epidemiology in a multiracial Asian country, Gastroenterology, 26(8):1333-7.

[Rappaport,1980], Rappaport AM.,(1980). Hepatic blood flow: morphologic aspects and physiologic regulation. Int Rev Physiol. 21:1-63.

[Ronald and Soille, 2018], Ronald Jones and Pierre Soille, (2018). Radial Decomposition of Disks and Spheres, Pattern Recognition Letters, 17(5):1057-1063.

[Soille P, 2013], Pierre Soille, (2013). Morphological Image Analysis; Principles and Applications, springer.

[Stasi et al, 2019], Stasi C, Tsochatzis EA, Hall A, Rosenberg W, Milani S, Dhillon AP, Pinzani M, (2019),Comparison and correlation of fibrosis stage assessment by collagen proportionate area (CPA) and the ELF panel in patients with chronic liver disease, Dig Liver Dis.PMID: 30606698

[Velleman and Hoaglin,1981], Velleman, P.F., and D.C. Hoaglin.,(1981) Applications, Basics, and Computing of Exploratory Data Analysis. Pacific Grove, CA: Duxbury Press.

[Wang et al 2019],Wang H, Fu J, Qi X, Sun J, Chen Y. , (2019) , Laparoscopic totally extraperitoneal (TEP) inguinal hernia repair in patients with liver cirrhosis accompanied by ascites, Medicine Baltimore PMID: 31651835.

[Zhou et. al, 2019], Zhou W. C., Z hang Q. B., Qiao L.,(2019). Pathogenesis of liver cirrhosis, World Journal of Gastroenterology,WJG,20(23):7312-7324.